

The Influence of Mineralization on Intratrabecular Stress and Strain Distribution in Developing Trabecular Bone

LARS MULDER, LEO J. VAN RUIJVEN, JAN HARM KOOLSTRA, and THEO M. G. J. VAN EIJDEN

Department of Functional Anatomy, Academic Centre for Dentistry Amsterdam (ACTA), Universiteit van Amsterdam and Vrije Universiteit, Meibergdreef 15, Amsterdam 1105 AZ, The Netherlands

(Received 5 December 2006; accepted 20 June 2007; published online 29 June 2007)

Abstract—The load-transfer pathway in trabecular bone is largely determined by its architecture. However, the influence of variations in mineralization is not known. The goal of this study was to examine the influence of inhomogeneously distributed degrees of mineralization (DMB) on intratrabecular stresses and strains. Cubic mandibular condylar bone specimens from fetal and newborn pigs were used. Finite element models were constructed, in which the element tissue moduli were scaled to the local DMB. Disregarding the observed distribution of mineralization was associated with an overestimation of average equivalent strain and underestimation of von Mises equivalent stress. From the surface of trabecular elements towards their core the strain decreased irrespective of tissue stiffness distribution. This indicates that the trabecular elements were bent during the compression experiment. Inhomogeneously distributed tissue stiffness resulted in a low stress at the surface that increased towards the core. In contrast, disregarding this tissue stiffness distribution resulted in high stress at the surface which decreased towards the core. It was concluded that the increased DMB, together with concurring alterations in architecture, during development leads to a structure which is able to resist increasing loads without an increase in average deformation, which may lead to damage.

Keywords—Mandibular condyle, Trabecular bone, Mechanical properties, FE models, Development.

INTRODUCTION

The trabecular bone of the mandibular condyle is considered to transfer a multitude of mechanical loads, applied to the relatively thin subchondral bone, to the cortical shell of the mandibular ramus. The load-transfer pathway is largely determined by the architecture and local stiffness of the trabecular bone. During early development, the condyle is increasingly

loaded due to involuntary contraction of developing muscles.⁸ Owing to this loading, the trabecular elements are subjected to strain, which leads to stress in the bone tissue. Both stress and strain are considered to modulate the growth of the bone.² Due to this mechanism, bone is able to adapt to a changing mechanical environment during development. This may result, at the stage of birth, in a structure that is able to adequately withstand the forces that go along with early feeding behavior.

Over the past few years finite element (FE) analysis based on micro-computed tomography (microCT) reconstructions has become a powerful tool for determining the apparent mechanical properties of selected trabecular bone volumes^{28,32} or even complete bones.^{12,24,29,34} In many cases these analyses have replaced physical mechanical tests where these were unfeasible or even impossible to perform. They can be used to predict the apparent mechanical properties of some volume of interest composed of irregularly shaped trabeculae. In addition to apparent mechanical properties, local strains and stresses within the trabeculae can be estimated.

The results of FE studies are heavily dependent on the assumed mechanical properties of the applied materials. Regarding bone tissue, these properties depend on the degree and distribution of mineralization. It has been shown that mineralization is not homogeneously distributed over the trabecular bone tissue of, for example, developing bone (pig mandible^{18,19}) and mature bone (rabbit femur¹; human mandibular condyle³³). The degree of mineralization appears to increase systematically from the surface of the trabeculae towards their centers. In recent studies, differences in degree of mineralization at the trabecular level have been demonstrated to be related with concomitant differences in mechanical properties.^{25,26} The resulting inhomogeneity of tissue stiffness can affect the apparent mechanical properties of the complete trabecular structure.^{1,13,27,33} Thus far, the effect of the

Address correspondence to Lars Mulder, Department of Functional Anatomy, Academic Centre for Dentistry Amsterdam (ACTA), Universiteit van Amsterdam and Vrije Universiteit, Meibergdreef 15, Amsterdam 1105 AZ, The Netherlands. Electronic mail: lars.mulder@amc.uva.nl

true distribution of mineralization has insufficiently been taken into account as a determinant of bone mechanical properties. It is unknown what the biomechanical consequences of these variations in mineralization are for the apparent biomechanical behavior of trabecular bone and for intratrabeular distributions of stresses and strains, and herewith how they change during development.

Quantitative knowledge about the three-dimensional intratrabeular tissue stress and strain distributions provides information on the nature of trabecular deformation during loading. It could, furthermore, be a key factor to quantify bone integrity according to Wolff's trajectorial hypothesis, which suggests that, normally, stress and strains should be distributed rather evenly over the trabecular structure. It may additionally give insights into micro-crack initiation and propagation behavior, which is influenced considerably by heterogeneity in bone mineralization.⁴ It may, furthermore, provide information about stimuli that are the bases for modeling and remodeling of bone tissue. Finally, knowledge regarding the development of mechanical properties during development will augment the understanding of normal trabecular bone development.

The goal of this study is, therefore, two-fold. First, to investigate how variations in distribution of mineralization in the mandibular condyle affect the biomechanical behavior both locally, i.e. intratrabeular distribution of stresses and strains, and globally, i.e. average stress and strain over the trabecular structure on an apparent level. Second, to investigate how these are altered during development.^{18,19}

To pursue these goals, finite element models of specimens from the mandibular condyle of developing pigs were analyzed. Their geometry had been modeled according to high-resolution microCT reconstructions (Fig. 1). The tissue stiffness was approximated from the local degree of mineralization, as measured also by microCT. The influence of the inhomogeneity of mineral distribution was analyzed by comparing the results with those of simulations where this inhomogeneity was neglected. The distribution of stresses and strains was assessed in a simulated compression test, applied along the vertical condylar axis.

MATERIALS AND METHODS

Samples

The mandibular condyles of four fetal and four newborn pigs from different litters (standard Dutch commercial hybrid race) were examined. The fetal specimens (estimated age: 75 days of gestation, mean

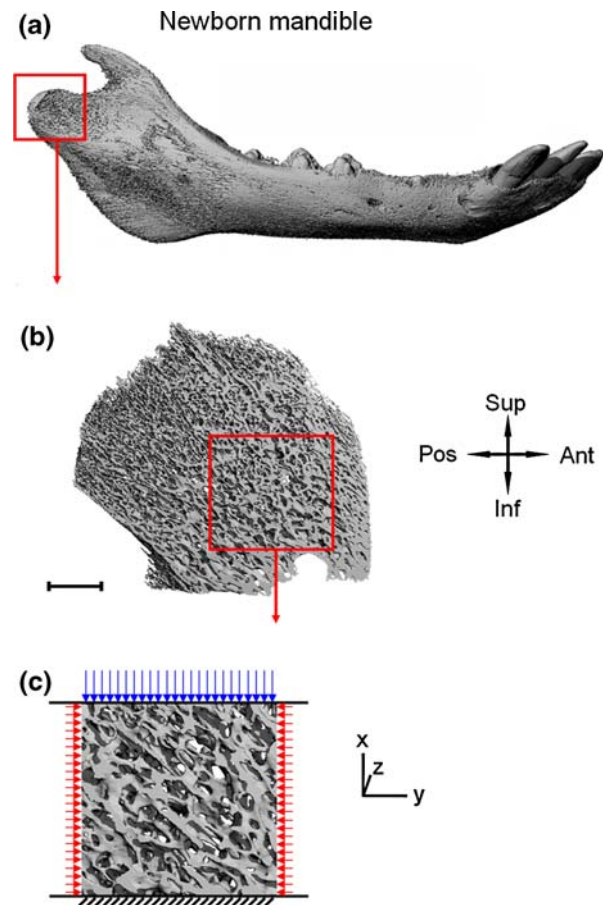


FIGURE 1. FE model and boundary conditions shown for a newborn mandible. (a) lateral view of a microCT reconstruction of a newborn pig mandible. (b) Sagittal cross-section of the mandibular condyle. The red square indicates the approximate location of the selected volume of interest. (c) Trabecular bone cube used for vertical compression simulation. Blue arrows: prescribed displacement on the top face. Red arrows: the displacements of nodes at the vertical surfaces were suppressed in the direction normal to the face. Black hatching: the bottom surface was fixed. Bar: 1.0 mm.

weight: 375 g) were obtained from commercially slaughtered sows and their age was estimated from the mean weight of the litter using growth curves.⁹ The newborn specimens (approximately 112–115 days post conception, mean weight: 1351 g) were acquired from the experimental farm of the Faculty of Veterinary Medicine in Utrecht, the Netherlands, and were euthanized by an intravenous overdose of ketamine (Narcetan) after premedication. The experiments have been approved by the Committee for Animal Experimentation of the Faculty of Veterinary Medicine, Utrecht, the Netherlands. The specimens were stored at -20°C prior to assessment.

The mandibles were dissected from the heads and cut in half at the symphyseal region. The right halves were prepared for analysis. The condyle was separated

with a frontal cut at the mandibular notch and with a horizontal cut at the mandibular ramus parallel to the occlusal plane.

MicroCT

Three-dimensional reconstructions of the bony condylar structures were obtained by using a high-resolution microCT system (μ CT 40; Scanco Medical, Bassersdorf, Switzerland). The specimens were mounted in cylindrical specimen holders (polyetherimide; outer diameter: 20 mm, wall thickness: 1.5 mm) and secured with synthetic foam. The scans yielded an isotropic spatial resolution of 10 μ m. A 45 kV peak-voltage X-ray beam was used, which corresponds to an effective energy of approximately 24 keV.¹⁷ An integration time of 1200 ms was applied to reduce noise substantially and to facilitate the discrimination between bone and background. The microCT was equipped with an aluminum filter and a correction algorithm that sufficiently reduced the beam hardening artifacts to enable quantitative measurements of the degree and distribution of mineralization.¹⁷ The computed attenuation coefficient of the X-ray beam for each volume element (voxel) was stored in an attenuation map and represented by a gray value in the reconstruction.

Cubic volumes of interest were defined in the condyles (fetal: approximately 1.5 mm³, newborn: approximately 7.5 mm³), and were built up out of 10 \times 10 \times 10 μ m³ voxels from which degree of mineralization and architecture were determined (Fig. 1). The top and bottom plane of the cubes were oriented parallel to the occlusal plane. To discriminate between bone and background, the reconstructions were segmented using an adaptive threshold determination procedure, which was visually checked. In a segmented image every voxel with a linear attenuation value below the threshold (assumably representing soft tissue or background) was made transparent and voxels above this threshold (representing bone) kept their original gray value. The latter can be considered proportional to the local degree of mineralization of bone (DMB).²¹ The DMB is the mass density of bone tissue and is expressed as the mass of mineralized tissue (mg) relative to its volume (cm³) in a volume of interest after thresholding has been performed.

The DMB was quantified by comparing the attenuation coefficient with reference measurements of a phantom containing hydroxyapatite of 0, 200, 400, 600, and 800 mg/cm³. To investigate the radial distribution of the degree of mineralization in the trabeculae a so-called peeling algorithm was used. Consecutive layers of bone-containing voxels (7–8 μ m thick) were peeled from the trabeculae, going from their surface

inwards, towards the core. Voxels peeled from the trabecular surface may have either belonged to a surface that was horizontal or vertical. In those cases the average voxel thickness that was peeled off is 10 μ m. However, when voxels are peeled off that belong to a perfectly diagonal surface (possible in multiple directions), the average thickness of the peeled off layer is somewhere between 7.1 and 8.6 μ m. In a microCT reconstruction of trabecular bone, a mixture of differently oriented surfaces is present, of which most are angled to some degree. Therefore, the average thickness of a peeled off layer is about 7–8 μ m in our estimation. Bone-containing voxels were identified as surface voxels when minimally one of its six sides bordered on voxels that were identified as background. In this procedure, the bone voxels in the layer adjacent to the marrow space were disregarded as this layer is likely to be corrupted by partial volume effects. After a layer had been peeled off, its average degree and variation (SD) of mineralization were calculated. Subsequently, the voxels that were peeled off were replaced by background voxels. In this way consecutive layers were characterized until the entire trabecular structure and, thus, all bone-containing voxels were usurped. This leads to seven layers for the fetal specimens and nine for the newborns. Furthermore, the frequency distribution was analyzed. The entire range of DMB values present in a specific sample was divided in 100 bins. The frequency distribution was obtained by counting the number of voxels in such a bin. Indeed, the area under the curves sums to unity, due to normalization with the total number of voxels in the specific bone sample.

The trabecular architecture was quantified by a number of architectural variables (BV/TV: bone volume fraction, Tb.N: trabecular number, Tb.Th: trabecular thickness, Tb.Sp: trabecular separation (Scanco software 3.2, Scanco Medical AG).

FE Analyses

Using the three-dimensional reconstructions created with microCT, an FE model was created for every specimen. The voxels in the three-dimensional microCT reconstructions were directly converted into cubic eight-node brick elements. The tissue modulus (E_t) was approximated from the DMB value of the corresponding microCT voxel according to $\log E_t = -8.58 + 4.05 \cdot \log[\text{Ca}]$.⁷ The concentration of calcium [Ca], expressed as mg/g by Currey (1999) was recalculated to the concentration of hydroxyapatite [HA] or DMB by multiplying [Ca] by a factor 2.5 (approximately 40% of hydroxyapatite consists of calcium) and subsequently multiplying this by 1.4 g/cm³, i.e. the specific density of trabecular bone tissue.^{14,22} When the

inhomogeneous distribution of DMB was disregarded, all elements were equipped with the same tissue modulus, corresponding to the average DMB of that specimen.

The FE problems were solved using an element-by-element FE-solver.²⁹ This program was modified to permit the assignment of a different Young's modulus to each individual element. A uniaxial compression test, corresponding to the superoinferior direction, was simulated by applying a uniform displacement (1%) on the superior surface of the specimen cubes (Fig. 1). Displacements of nodes at the other surfaces were suppressed in the direction normal to the face. The vertical direction was assumed to correspond most closely to the average joint loading direction.

From the resulting components of the strain and stress tensor, the average equivalent strain and von Mises equivalent stress were calculated, respectively, based on the fact that plastic deformation, which relates to the risk of failure, is essentially shear deformation which entails no volume changes. Therefore, especially the parts of the strain and stress tensor that belong to the shear component were considered. The definition which was applied to calculate the equivalent strain and von Mises equivalent stress was as follows:

$$\varepsilon_{eq} = \sqrt{\frac{1}{2} \left((\varepsilon_{xx} - \varepsilon_{yy})^2 + (\varepsilon_{yy} - \varepsilon_{zz})^2 + (\varepsilon_{zz} - \varepsilon_{xx})^2 + 6 \cdot (\varepsilon_{yz}^2 + \varepsilon_{xz}^2 + \varepsilon_{xy}^2) \right)}$$

$$\sigma_{eq} = \sqrt{\frac{1}{2} \left((\sigma_{xx} - \sigma_{yy})^2 + (\sigma_{yy} - \sigma_{zz})^2 + (\sigma_{zz} - \sigma_{xx})^2 + 6 \cdot (\sigma_{yz}^2 + \sigma_{xz}^2 + \sigma_{xy}^2) \right)}$$

Frequency distributions of the variables mentioned and of the component of principal strain with the largest magnitude were constructed. The radial distribution of the equivalent strain and von Mises equivalent stress in the trabecular elements was studied by applying a similar peeling algorithm as applied for the DMB.

Statistics

To analyze the results from the peeling algorithm, a general linear model (repeated measures) was applied. To study the difference between models per layer a general linear model (multivariate) was used. From the frequency distributions of the equivalent strain and von Mises equivalent stress, the mean and standard deviation of these variables were determined. Differences between fetal and newborn specimens were statistically

TABLE 1. Architectural variables of the trabecular bone in the condyle.

	Fetal mean (sd)	Newborn mean (sd)
BV/TV (%)	24.14 (4.14)	19.65 (1.64)
Tb.Th (mm)	0.049 (0.002) ^a	0.063 (0.005)
Tb.N (mm ⁻¹)	6.99 (0.47) ^a	3.95 (0.22)
Tb.Sp (mm)	0.122 (0.012) ^a	0.228 (0.016)

^a Significant difference between fetal and newborn specimens ($p < 0.01$).

BV/TV: bone volume fraction; Tb.Th: trabecular thickness; Tb.N: trabecular number; Tb.Sp: trabecular separation.

assessed using independent-sample *t*-tests. A *p* value of less than 0.05 was considered statistically significant.

RESULTS

Values for and differences in architectural variables between fetal and newborn stages are given in Table 1. Architectural development coincided with a reorganization of bone of the trabecular structure without a significant change in the bone volume fraction itself. There was an increase in trabecular thickness (from 0.049 to 0.063 mm) and separation (from 0.122 to

0.228 mm) with a concurring decrease in trabecular number (from 6.99 to 3.95 mm⁻¹).

The degree of mineralization significantly increased during development from fetal to newborn age. Whereas in fetal specimens the average DMB was approximately 630 mg/cm³, in the newborn specimens it was to approximately 730 mg/cm³ (Fig. 2a). The variation in mineralization as characterized by the width of the frequency distribution remained constant. The increase in DMB led to an increase in average tissue stiffness from fetal (approximately 4.0 GPa) to newborn (approximately 6.7 GPa) specimens, according to the model by Currey (1999). Using the peeling algorithm, it was demonstrated that the mineralization was distributed inhomogeneously in a systematic pattern over the trabecular elements (Fig. 2b). From the surface of trabeculae towards their core, the degree of

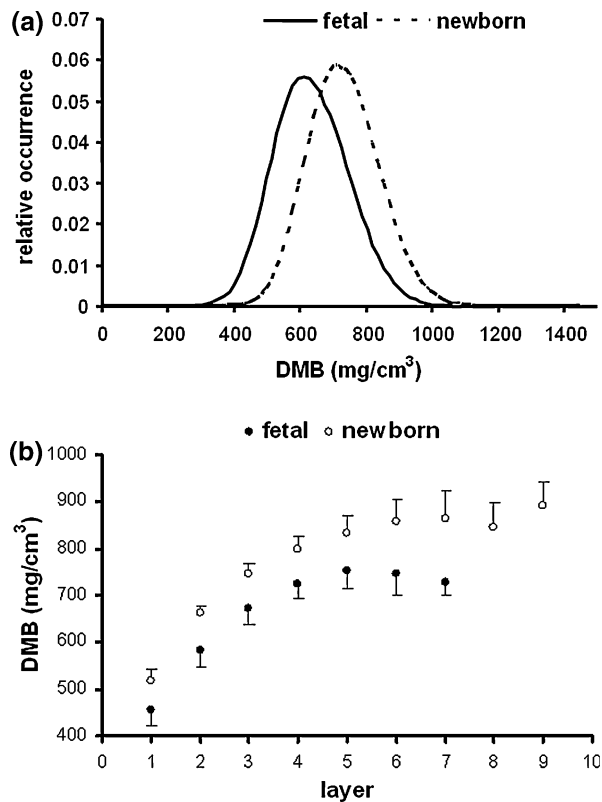


FIGURE 2. Distribution of degree of mineralization (DMB) in fetal ($n = 4$) and newborn ($n = 4$) trabecular bone specimens. (a) frequency distributions. Note the increase in average DMB from fetal to newborn (b) Distribution from the surface of trabecular elements (layer 1) to their cores (fetal: layer 7; newborn: layer 9). The error bars represent the standard deviation between the specimens in a specific group (fetal or newborn) for a peeled off layer. Layer 1 was omitted in calculations of average values and histograms.

mineralization increased significantly in both the fetal and newborn specimens. For the fetal ones, the second and third layers were statistically different from each other and successive layers ($p < 0.05$). The increase in DMB reached a plateau after the third layer as there was no difference between the more central layers. In the newborn ones, layers two through five were different from each other and successive layers ($p < 0.05$), whereas layers six through nine were

not significantly different and thus also reaching a plateau.

The average equivalent strain did not change significantly from fetal to newborn stages (Table 2). However, when the influence of mineralization on the tissue elasticity was disregarded, the average equivalent strain was overestimated by approximately 20% ($p < 0.01$). This was also noticeable from the frequency distributions (Fig. 3a) and detectable in the profile through trabecular elements as obtained by the peeling procedure. In both fetal and newborn specimens, the strain was largest in the superficial layers of the trabecular elements, and significantly reduced when getting closer to the cores (Figs. 3b–d), eventually leveling off towards the center of the trabecular elements. When the distribution of mineralization was disregarded, the equivalent strain was overestimated starting from layer three (fetal) and four (newborn).

The average values of the von Mises equivalent stress increased from fetal to newborn stages (Table 2). Also, the frequency distribution changed during development (Fig. 4a). In the newborn specimens the stresses with the most frequent occurrence were larger than in the fetal specimens. These stresses were reduced in value by approximately 16% when the influence of mineral distribution was disregarded (Table 2; Fig. 4a). This influence was also evident in the radial distribution of equivalent stress over the trabecular elements. It was shown that the highest stress occurred near their center (Fig. 4b). The profiles from both fetal (Fig. 4c) and newborn specimens (Fig. 4d) showed similar trends as examined by the peeling procedure. The surface of trabecular elements contained the lowest stress, which significantly increased to approximately halfway towards the cores and subsequently decreased again near the cores, but not reaching the values present at the surface. It was shown that disregarding the inhomogeneous distribution of mineralization resulted in a different profile; the highest stresses were then observed at the surface, which decreased towards the cores. It, thus, caused an overestimation of the equivalent stress at the surface of trabecular elements and an underestimation at their cores.

TABLE 2. Equivalent strain and stress.

	Fetal mean (sd)	Newborn mean (sd)
Equivalent microstrain, inhomogeneous model	440 (130)	510 (70)
Equivalent microstrain, homogeneous model	530 (140) ^c	620 (150) ^b
Equivalent stress, inhomogeneous model (MPa)	1.29 (0.38) ^a	2.53 (0.94)
Equivalent stress, homogeneous model (MPa)	1.08 (0.30) ^{ab}	2.16 (0.74) ^b

^a Significant differences between fetal and newborn specimens, $p < 0.05$.

^b Significant differences between the homogeneous and inhomogeneous model per variable, $p < 0.05$; ^c $p < 0.01$.

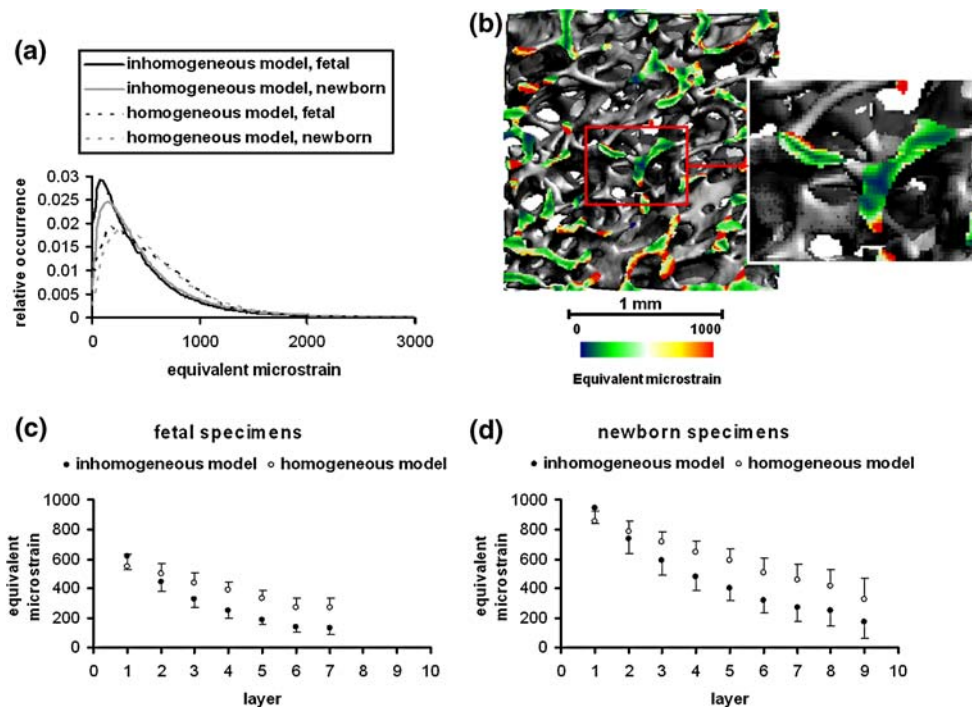


FIGURE 3. Distribution of equivalent strain in fetal ($n = 4$) and newborn ($n = 4$) specimens. The histograms do not contain surface voxels. (a) frequency distributions. Note the similarity between fetal and newborn specimens and the difference between the models. (b) Frontal cross-section of the cubic volume of interest of a newborn specimen. Note the decreasing trend of the equivalent strain from the trabecular surfaces to the cores (inset). (c) Three-dimensional distribution from the surface of fetal trabecular elements (layer 1) to their core (layer 7). (d) Three-dimensional distribution from the surface of newborn trabecular elements (layer 1) to their core (layer 9). The error bars represent the standard deviation between the specimens in a specific group (fetal or newborn) for a peeled off layer.

The distribution of the component of the principal strain with the largest magnitude (Fig. 5) was equally wide for the fetal and newborn specimens. However, distributions obtained while disregarding mineral distribution clearly overestimated the larger strains in compression. In both age groups the larger part of the component of the principal strain with the largest magnitude was compressive. The balance seemed to shift even more to compression in newborn specimens.

DISCUSSION

To our knowledge this is the first study in which the influence of mineral distribution, related to tissue stiffness, on the local distribution of tissue stress and strain over the trabecular bone has been investigated. We found that the cores of the trabeculae have higher mineralization than superficial regions. This indicates that modeling (formation of new bone without prior absorption of old bone tissue) and remodeling (replacement of old bone tissue with new bone) occurs predominantly at the trabecular surface. Consequently, the youngest bone is present at the surface and the oldest bone at the core of the trabeculae.

From a mechanical point of view, it should be noted that the bone mineral provides rigidity to the bone.⁶ Bone tissue with a high degree of mineralization, as found in the cores of trabecular elements, can be expected to be stiff but brittle, with a low failure energy.⁵ Less mineralized bone tissue, present at the trabecular surface, is more compliant and demonstrates a greater ability to undergo high strains. Moreover, due to the low degree of mineralization, the accompanying stress remains low. In the cores of trabecular elements, the high degree of mineralization may contribute to the rigidity of the bone which leads to low strains, but high stress. From that perspective, heterogeneity in bone mineralization may have a considerable influence on the bone toughness⁴ and may make the trabeculae compliant to bending.

This composition may, furthermore, be considered preferable to prevent crack propagation. Cracks initiated in the highly mineralized tissue of the trabecular cores might in this way be prevented from continuing to the surface layers, which have lower a degree of mineralization.³⁵ This prevents complete fracture of the trabecular elements and enables repair of the damage. This is confirmed by observation of damaged trabecular elements, where the highly mineralized core

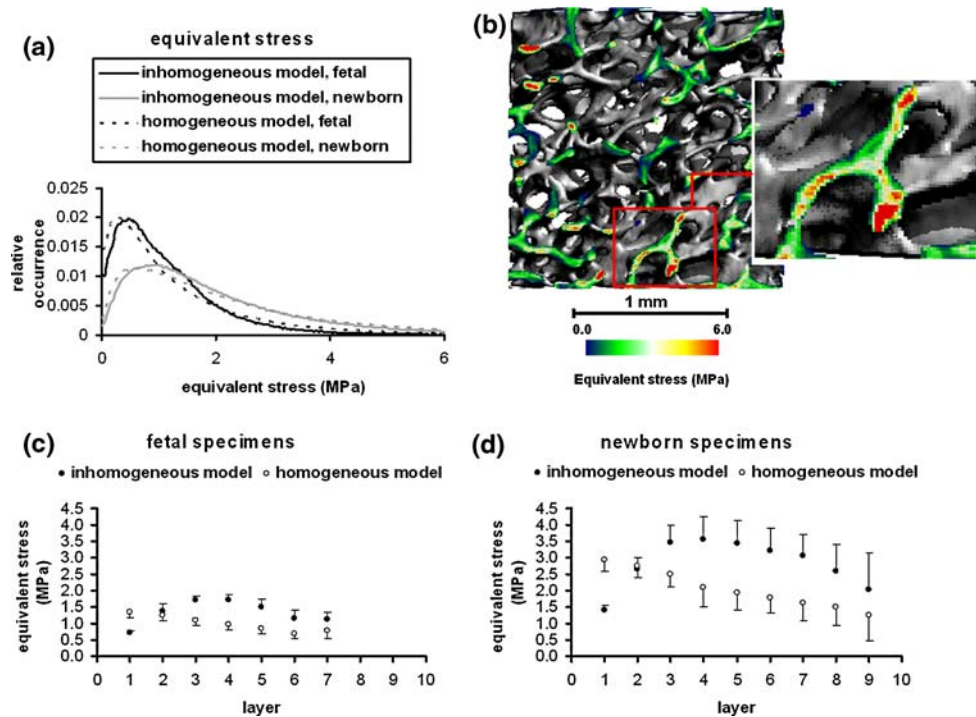


FIGURE 4. Distribution of equivalent stress in fetal ($n = 4$) and newborn ($n = 4$) specimens. (a) frequency distributions. Note the difference between fetal and newborn specimens and the difference between the models. (b) Frontal cross-section of the cubic volume of interest of a newborn specimen. Note the increasing trend of the equivalent stress from the trabecular surfaces to the cores (inset). (c) Three-dimensional distribution from the surface of fetal trabecular elements (layer 1) to their core (layer 7). (d) Three-dimensional distribution from the surface of newborn trabecular elements (layer 1) to their core (layer 9). The error bars represent the standard deviation between the specimens in a specific group (fetal or newborn) for a peeled off layer.

contains microcracks, while the mechanical integrity of the trabecular elements is maintained by the undisturbed, less mineralized surface.^{10,16} However, the fact that microcracks are observed mostly in the trabecular cores, may be due to the remodeling process, which occurs at the trabecular surface and may explain the absence of cracks in this region. Also, stress concentrations in surface features, such as trabecular junctions and resorption cavities may contribute to the formation of cracks at trabecular surfaces. Further detailed fracture/damage mechanics analyses are required to fully investigate this question.

We found that incorporating inhomogeneously distributed tissue stiffness, according to the local degree of mineralization, had a profound effect on frequency distributions and three-dimensional profiles of stress and strain through trabecular elements. Disregarding this inhomogeneously distributed tissue stiffness was demonstrated to lead to an overestimation in average equivalent strain, with vertical compression. The von Mises equivalent stress on the other hand was underestimated in that case. If the compression test were a load controlled test, the results may be similar. It has been shown that incorporating the inhomogeneously distributed mineralization leads to a decrease in apparent/structural stiffness of about 10%.²⁰ This

would imply that in a load control test the inhomogeneous model will be compressed 10% more than the homogeneous one. From Table 2 it can be deduced that the average strain during a strain controlled test was 20% lower in the inhomogeneous model. As a consequence, one may expect a 10% lower average strain in the inhomogeneous model during a load control test in comparison to the homogeneous model.

The three-dimensional stress and strain profile through the trabecular elements indicates that the deformation scheme of trabecular elements during loading is affected by the distribution of mineralization. Higher strains at the surface of trabecular elements than in the cores indicate that numerous trabecular elements undergo bending deformation. However, in pure bending the amount of compressed and stretched tissue would be equal, which is not the case for the presently applied deformation which results in more compression than tension (see Fig. 5). This signifies that not all the trabecular elements undergo pure bending during a compression test. This might be dependent on the orientation of the trabecular elements with respect to the loading direction and the distribution of mineralization. Furthermore, besides trabecular elements there may also be other structures, as the bone forming the connections

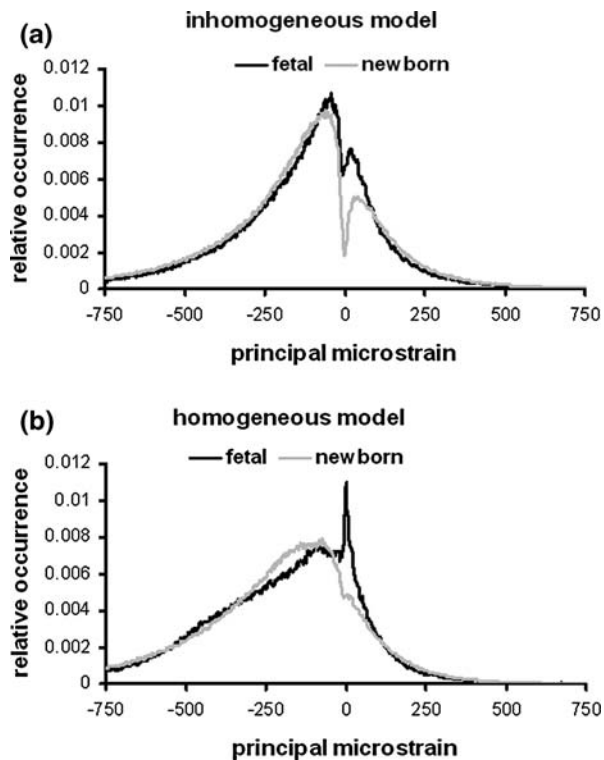


FIGURE 5. Frequency distributions of the principal strain with the largest magnitude for fetal ($n = 4$) and newborn ($n = 4$) specimens. (a) inhomogeneous models. (b) homogeneous models.

between the trabeculae display a certain loading pattern, which might not be bending. However, the general bending deformation of the trabecular elements was profound enough for it to be visible in the intratrabeular distribution of equivalent strain. The dip in principal strain around zero strain was expected, as in a correctly applied load, one can expect all the elements to be either stretched or compressed. Its occurrence, however, depends on the bin width that was chosen to create the frequency distributions.

According to Wolff's law, the trabecular architecture is assumed to minimize both bone stress and weight. The present study, however, does not confirm this paradigm that, normally, stress and strains should be distributed rather evenly over the trabecular architecture. In contrast, it is in agreement with previous studies where frequency distributions in human and canine femurs were of similar shape.^{30,31} The fact that no uniform distributions of stress and strain were found is probably due to the fact that both the bone architecture and mineralization are adapted to multiple loading directions. Moreover, an optimal trabecular structure may appear differently under multi-directional loads than the 'trajectorial' organization proposed by Wolff.²³ Obviously, a perfectly even distribution cannot be expected for one single

load case because the condyle is subjected to varying loading magnitudes and directions during normal use. Not only joint forces but also muscle forces are applied on it. A trabecular structure created through load adaptive remodeling should reflect all these different loading configurations in a weighted manner.³¹

With the development from fetal to newborn, the distribution of the equivalent strain as a result of the applied compression did not change. Between the stages a similar frequency distribution and profile through trabecular elements was observed. However, an increased amount of stress, probably due to the increase in DMB was found. This increase was not accompanied by a change in the profiles through trabecular elements. Between these stages, changes in trabecular architecture, without altering the bone volume fraction has occurred.^{18,19} These changes included an increase in thickness of the trabecular elements, a reduction in their numbers, and a doubling of the intertrabeular spacing (Table 1). Furthermore, the average DMB had increased. These phenomena together show us that the increased DMB leads to a structure which is able to resist larger amounts of load without an increase in average deformation.

In the present analysis, a number of simplifications have been applied. First, in the calculation of the average values for DMB and equivalent stress and strain the superficial bone layer was disregarded. This was done because the superficial voxels are likely to be corrupted by partial volume effects. Their inclusion would have led to an underestimation of mean DMB as they will have a DMB less than this average. Second, the material property of the bone tissue in our model was assumed to be isotropic and linearly elastic. The latter is applicable for trabecular bone for small deformations.¹⁵ Third, trabecular bone tissue has a preferred orientation which makes it both spatially and mechanically anisotropic.²⁶ This means that bone tissue properties may vary when different loading directions are applied. Fourth, the exponential relation used to scale tissue stiffness from local degree of mineralization was derived from experiments using cortical bone samples from several species.⁷ Although it is very likely that a similar relation will be valid in pig trabecular bone tissue, it is unknown if and how these fit into this relationship. A possible aberration from this relationship, however, does presumably not affect the findings in a qualitative sense as it is not likely that the proportional character of the relationship will be affected. Finally, the trabecular bone has been modeled morphologically by cubic elements. This approach produces 'jagged' surfaces. It has been shown that this can lead to local computational oscillations and errors in the stress-strain calculations, near these surfaces.^{3,11} Because the surface layer was omitted in the determination of the histograms, the

effect on the histograms and the calculated average and standard deviation will be small.³⁰ Furthermore, due to averaging the results over neighboring elements, possible instabilities were reduced.¹¹

It can be concluded that the inhomogeneous distribution of mineralization has a decreasing effect on the average equivalent strain, while it tends to raise the von Mises equivalent stress in the trabecular bone. The equivalent strain was largest at the surface of trabecular elements and decreased towards their core. The equivalent stress was found to have its maximum about halfway between the surface and the core. This indicates that the trabecular elements are bent during a compression experiment. No changes in equivalent strain were observed during development from fetal to newborn specimens, but equivalent stress increased. The profiles from surface to core were similar between fetal and newborn specimens. Incorporating inhomogeneously distributed tissue stiffness, scaled to the local degree of mineralization, in FE models is essential for a better understanding of bone mechanical behavior.

ACKNOWLEDGEMENTS

Appreciation goes out to Bert van Rietbergen from the Department of Biomedical Engineering, Eindhoven University of Technology, Eindhoven, The Netherlands, for his assistance with the inhomogeneous finite element models. The authors would also like to thank Geerling Langenbach for critically reading the manuscript. This research was institutionally supported by the Inter-University Research School of Dentistry, through the Academic Centre for Dentistry Amsterdam.

REFERENCES

- ¹Bourne, B. C., and M. C. H. van der Meulen. Finite element models predict cancellous apparent modulus when tissue modulus is scaled from specimen CT-attenuation. *J. Biomech.* 37:613–621, 2004.
- ²Burger, E. H., J. Klein-Nulend, and J. P. Veldhuijzen. Modulation of osteogenesis in fetal bone rudiments by mechanical stress in vitro. *J. Biomech.* 24:101–109, 1991.
- ³Camacho, D. L., R. H. Hopper, G. M. Lin, and B. S. Myers. An improved method for finite element mesh generation of geometrically complex structures with application to the skullbase. *J. Biomech.* 30:1067–1070, 1997.
- ⁴Ciarelli, T. E., D. P. Fyhrie, and A. M. Parfitt. Effects of vertebral bone fragility and bone formation rate on the mineralization levels of cancellous bone from white females. *Bone* 32:311–315, 2003.
- ⁵Currey, J. D. Effects of differences in mineralization on the mechanical properties of bone. *Philos. Trans. R. Soc. Lond. B Biol. Sci.* 304:509–518, 1984.
- ⁶Currey, J. D. The effect of porosity and mineral content on the Young's modulus of elasticity of compact bone. *J. Biomech.* 21:131–139, 1988.
- ⁷Currey, J. D. What determines the bending strength of compact bone? *J. Exp. Biol.* 202:2495–2503, 1999.
- ⁸de Vries, J. I. P., G. H. A. Visser, and H. F. R. Prechtl. The emergence of fetal behaviour. II. Quantitative aspects. *Early Hum. Dev.* 12:99–120, 1985.
- ⁹Evans, H. E., and W. O. Sack. Prenatal development of domestic and laboratory mammals: Growth curves, external features and selected references. *Zentralbl. Veterinarmed. [C]* 2:11–45, 1973.
- ¹⁰Fyhrie, D. P., and M. B. Schaffler. Failure mechanisms in human vertebral cancellous bone. *Bone* 15:105–109, 1994.
- ¹¹Guldborg, R. E., S. J. Hollister, and G. T. Charras. The accuracy of digital image-based finite element models. *J. Biomech. Eng.* 120:289–295, 1998.
- ¹²Homminga, J., B. van Rietbergen, E. M. Lochmüller, H. Weinans, F. Eckstein, and R. Huiskes. The osteoporotic vertebral structure is well adapted to the loads of daily life, but not to infrequent "error" loads. *Bone* 34:510–516, 2004.
- ¹³Jaasma, M. J., H. H. Bayraktar, G. L. Niebur, and T. M. Keaveny. Biomechanical effects of intraspecimen variation in tissue modulus for trabecular bone. *J. Biomech* 35:237–246, 2002.
- ¹⁴Kabel, J., B. van Rietbergen, M. Dalstra, A. Odgaard, and R. Huiskes. The role of an effective isotropic tissue modulus in the elastic properties of cancellous bone. *J. Biomech.* 32:673–80, 1999.
- ¹⁵Keaveny, T. M., X. E. Guo, E. F. Wachtel, T. A. McMahon, and W. C. Hayes. Trabecular bone exhibits fully linear elastic behaviour and yields at low strains. *J. Biomech.* 27:1127–1136, 1994.
- ¹⁶Mori, S., R. Harruf, W. Ambrosius, and D. B. Burr. Trabecular bone volume and microdamage accumulation in the femoral heads of women with and without femoral neck fractures. *Bone* 21:521–526, 1997.
- ¹⁷Mulder, L., J. H. Koolstra, and T. M. G. J. van Eijden. Accuracy of microCT in the quantitative determination of the degree and distribution of mineralization in developing bone. *Acta Radiol.* 45:769–777, 2004.
- ¹⁸Mulder, L., J. H. Koolstra, W. A. Wejjs, and T. M. G. J. van Eijden. Architecture and mineralization of developing trabecular bone in the pig mandibular condyle. *Anat. Rec. A Discov. Mol. Cell. Evol. Biol.* 285:659–667, 2005.
- ¹⁹Mulder, L., J. H. Koolstra, H. W. de Jonge, and T. M. G. J. van Eijden. Architecture and mineralization of developing cortical and trabecular bone of the mandible. *Anat. Embryol.* 211:71–78, 2006.
- ²⁰Mulder, L., L. J. van Ruijven, J. H. Koolstra, and T. M. G. J. van Eijden. Biomechanical consequences of developmental changes in trabecular architecture and mineralization of the pig mandibular condyle. *J. Biomech.* 40:1575–1582, 2007.
- ²¹Nuzzo, S., C. Meneghini, P. Braillon, R. Bouvier, S. Mobilio, and F. Peyrin. Microarchitectural and physical changes during fetal growth in human vertebral bone. *J. Bone Miner. Res.* 18:760–768, 2003.
- ²²Ouyang, J., G. T. Yang, W. Z. Wu, Q. A. Zhu, and S. Z. Zhong. Biomechanical characteristics of human trabecular bone. *Clin. Biomech.* 12:522–524, 1997.
- ²³Pidaparti, R. M., and C. H. Turner. Cancellous bone architecture: advantages of nonorthogonal trabecular alignment under multidirectional joint loading. *J. Biomech.* 26:111–119, 1997.

- ²⁴Pistoia, W., B. van Rietbergen, E. M. Lochmüller, C. A. Lill, F. Eckstein, and P. Rügsegger. Estimation of distal radius failure load with micro-finite element analysis models based on three-dimensional peripheral quantitative computed tomography images. *Bone* 30:842–848, 2002.
- ²⁵Rho, J. Y., T. Y. Tsui, and G. M. Pharr. Elastic properties of human cortical and trabecular lamellar bone measured by nanoindentation. *Biomaterials* 18:1325–1330, 1997.
- ²⁶Roy, M. E., J. Y. Rho, T. Y. Tsui, N. D. Evans, and G. M. Pharr. Mechanical and morphological variation of the human lumbar vertebral cortical and trabecular bone. *J. Biomed. Mater. Res.* 44:191–197, 1999.
- ²⁷van der Linden, J. C., D. H. Birkenhäger-Frenkel, J. A. N. Verhaar, and H. Weinans. Trabecular bone's mechanical properties are affected by its non-uniform mineral distribution. *J. Biomech.* 34:1573–1580, 2001.
- ²⁸van Eijden, T. M. G. J., L. J. van Ruijven, and E. B. W. Giesen. Bone tissue stiffness in the mandibular condyle is dependent on the direction and density of the cancellous structure. *Calcif. Tissue Int.* 75:502–508, 2004.
- ²⁹van Rietbergen, B., H. Weinans, R. Huiskes, and A. Odgaard. A new method to determine trabecular bone elastic properties and loading using micromechanical finite-element models. *J. Biomech.* 28:69–81, 1995.
- ³⁰van Rietbergen, B., R. Müller, D. Ulrich, P. Rügsegger, and R. Huiskes. Tissue stresses and strain in trabeculae of a canine proximal femur can be quantified from computer reconstructions. *J. Biomech.* 32:165–173, 1999.
- ³¹van Rietbergen, B., R. Huiskes, F. Eckstein, and P. Rügsegger. Trabecular bone tissue strains in healthy and osteoporotic human femur. *J. Bone Miner. Res.* 18:1781–1788, 2003.
- ³²van Ruijven, L. J., E. B. W. Giesen, M. Farella, and T. M. G. J. van Eijden. Prediction of mechanical properties of the cancellous bone of the mandibular condyle. *J. Dent. Res.* 82:819–823, 2003.
- ³³van Ruijven, L. J., L. Mulder, and T. M. G. J. van Eijden. Variations in mineralization affect the stress and strain distributions in cortical and trabecular bone. *J. Biomech.* 40:1211–1218, 2007.
- ³⁴Verhulp, E., B. van Rietbergen, and R. Huiskes. Comparison of micro-level and continuum-level voxel models of the proximal femur. *J. Biomech.* 39:2951–2957, 2006.
- ³⁵Ziopoulos, P., and J. D. Currey. The extent of microcracking and the morphology of microcracks in damaged bone. *J. Mater. Sci.* 29:978–986, 1994.